Midgap states and charge inhomogeneities in corrugated graphene

F. Guinea[1]
[1] *Instituto de Ciencia de Materiales de Madrid (CSIC), Cantoblanco, Madrid 28049, Spain*

M. I. Katsnelson[2]
[2] *Condensed Matter Theory, Institute for Molecules and Materials, Radboud University Nijmegen, Toernoooiveld 1, NL-6525 ED Nijmegen, The Netherlands*

M. A. H. Vozmediano[3]
[3] *Instituto de Ciencia de Materiales de Madrid (CSIC), Cantoblanco, Madrid 28049, Spain*

We study the changes induced by the effective gauge field due to ripples on the low energy electronic structure of graphene. We show that zero energy Landau levels will form, associated to the smooth deformation of the graphene layer, when the height corrugation, h, and the length of the ripple, l, are such that $h^2/(la) \gtrsim 1$, where a is the lattice constant. The existence of localized levels gives rise to a large compressibility at zero energy, and to the enhancement of instabilities arising from electron-electron interactions including electronic phase separation. The combined effect of the ripples and an external magnetic field breaks the valley symmetry of graphene leading to the possibility of valley selection.

PACS numbers: 73.21.-b; 73.20.Hb; 73.22.-f

INTRODUCTION.

The discovery of atomic thick graphene layers[1], and the measurement of their novel electronic properties[2] have led to a great deal of interest. The details of the structure of these layers is not completely elucidated, although there is clear evidence that free standing sheets are not flat[3], and layers placed on an insulating substrate seem also not to be flat, following the corrugation of the susbtrate[4, 5]. The height and width of the observed ripples in free standing samples are consistent with models which take into account the tendency of carbon ions to form different types of bonds[6].

The intrinsic curvature of the graphene sheets[7, 8, 9, 10, 11], the modulation of hoppings by elastic strains[12, 13, 14], and hybridization between the π and σ bands induced by curvature[15] enter into the effective Dirac equation which describes the low energy electron states as a deformation induced gauge field. In the absence of scattering between the two inequivalent valleys in the Brillouin Zone, these gauge fields change the phases of coherent electrons, and can play a role similar to that of an effective magnetic field[9, 13, 16, 17, 18, 19], changing the transport properties of the system in the presence of low (real) magnetic fields.

Single layer graphene also shows inhomogeneities in the electronic distribution near half filling[2, 20]. These inhomogeneities may be related to the existence of ripples[11, 15].

In the present work, we study the changes induced by the effective gauge field due to ripples on the low energy electronic structure of graphene. These changes become important when the effective magnetic length due to the ripples is comparable to the ripple size. Then, zero energy Landau levels[21] can exist in regions where the effective field changes slowly. These midgap states are not suppressed by the off diagonal disorder associated to the ripples[22], and lead to a peak in the density of states at zero energy. While clean graphene is a semimetal, with a vanishing electronic compressibility at half filling, the existence of ripples lead to a large compressibility at zero energy, and to the enhancement of instabilities arising from electron-electron interactions. Note that zero gap states are expected when the flux of the effective magnetic field is larger than one in a given region[23]. It has also been shown that a sufficiently strong random gauge field leads to a divergent density of states at zero energy[24].

We present estimates of the strength of the effective field induced by ripples of the sizes observed experimentally, and discuss simple models which illustrates the formation of Landau levels as function of the deformation of the graphene layer. We also analyze the combined effects of ripples and a real magnetic field, showing that the equivalence of the two valleys in the Brillouin Zone of graphene is broken. We finally discuss possible instabilities which can arise due to the enhanced electronic compressibility, including the possibility of electronic phase separation. The Appendix describes simple models where the phenomena discussed in the paper can be studied analytically.

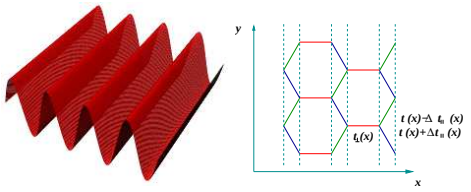

FIG. 1: (Color online). Left: sketch of the ripples considered in the text. Right: Modifications of the nearest neighbor hoppings induced by the ripple. See text for details.

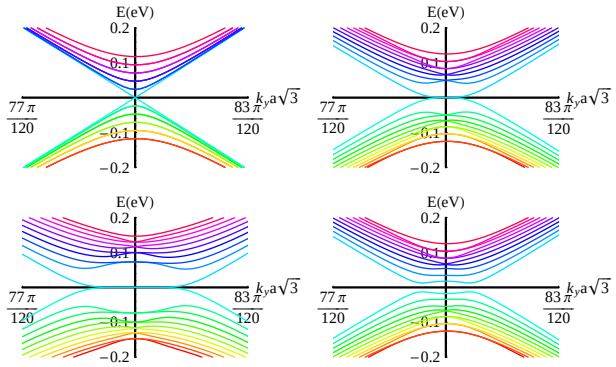

FIG. 2: (Color online). Low energy states induced by a ripple as shown in Fig.[1]. The average hopping is $t_{\|} = 3$eV. The width of the ripple is $1200a = 168$nm. The modulations of the hoppings are: Top left, $\delta t/t = 0$, top right, $\delta t/t = 0.02$, bottom left, $\delta t/t = 0.04$, bottom right, $\delta t/t = 0.02$, and a periodic electrostatic potential of amplitude 0.02eV.

EFFECTIVE GAUGE FIELD IN SINGLE LAYER GRAPHENE.

Qualitative estimates.

Fluctuations of order Δt of the hopping parameter t around an hexagon of the honeycomb lattice give rise to an effective flux, in units of eh/c, through the hexagon of order $\Delta\Phi \sim \Delta t/t$. If the hopping varies smoothly over a distance l, then $\Delta t \approx \delta t(a/l)$, where δt is the overall modulation of t, and a is a distance comparable to the lattice spacing. Then, the total flux in an region of area l^2 is $\Phi \sim (\delta t/t)(l/a)$. This number is also an estimate of the number of Landau levels with $n = 0$ within that area. Finally, the magnetic length associated with the effective field is $l_B \sim \sqrt{(t/\delta t)(la)}$, and the separation between the $n = 0$ and $n = \pm 1$ Landau levels is $\sqrt{(t\delta t)(a/l)}$. If the origin of the modulation δt is solely due to the strains induced by a ripple of height h and length l, then $\delta t \approx \partial \log(t)/\partial \log(d_{C-C}) h^2/(al)$, where $d_{C-C} \sim a$ is the length of the bond between nearest carbon atoms. In graphene, the parameter $\beta = \partial \log(t)/\partial \log(d_{C-C})$ is $\beta \approx 2$. Hence, we find that the flux per ripple, in quantum units, is:

$$\Phi \approx \beta \frac{h^2}{la} \tag{1}$$

For $h \sim 1 - 5$nm and $l \sim 50$nm, we find $\delta t/t \sim \delta v_{\rm F}/v_{\rm F} \sim 10^{-2} - 10^{-1}$, and $\Phi \gtrsim 1$.

One dimensional ripples.

We analyze numerically the emergence of midgap states as function of the modulations of the hoppings using a simple model with the geometry sketched in Fig.[1].This translational symmetry along the y axis greatly simplifies the calculations. The changes in the electronic structure induced by the ripple are determined by the local value of the gradient of the tight binding hoppings. More complicated patterns of ripples can be decomposed in regions described by an average gradient of the hoppings. Hence, the model studied here should have similar features to other structures, provided that the magnitude of the gradients of the hoppings are comparable.

The translational invariance along the y axis implies that k_y is a good quantum number. Hence, the hamiltonian can be reduced to a set of effective one dimensional hamiltonians, one for each value of k_y, which describe the hoppings between the rows shown on the right side of Fig.[1]. In the absence of modulations, the absolute values of these hoppings are t and $2t\cos(k_y\sqrt{3}a/2)$, were a is the distance between carbon atoms. The low energy states are centered around $k_y\sqrt{3}a = 2\pi/3$ and $k_y\sqrt{3}a = 4\pi/3$. The modulation of the hoppings leads to the replacement:

$$\begin{aligned} t &\leftrightarrow t_{\|}(x) \\ 2t\cos(\phi) &\leftrightarrow \sqrt{t_{\perp}^2(x)\cos^2(\phi) + \Delta t_{\perp}^2(x)\sin^2(\phi)} \end{aligned} \tag{2}$$

where $\phi = (\sqrt{3}k_y a)/2$. An external (real) magnetic field, described by the vector potential $A_y(x) = Bx$ leads to the replacement of k_y by $k_y + eA_y/c$.

We have calculated the bands of the ribbons shown in Fig.[1] using the modulation:

$$t_{\perp}(x) = \delta t \sin\left(\frac{2\pi x}{l}\right) \tag{3}$$

Results are shown in Fig.[2], with $l = 1200a$ (800 unit cells). Periodic boundary conditions are used. The plot corresponds to one of the valleys. The levels in the two valleys, in the absence of an external magnetic field, remain degenerate.

The calculations are consistent with the qualitative estimates made above. The number of midgap states is proportional to the range of k_y values where they are

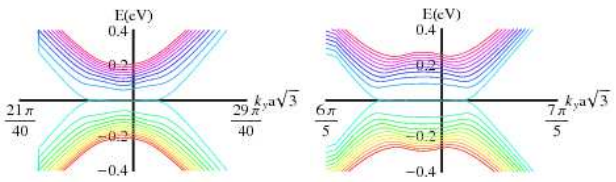

FIG. 3: (Color online). As in Fig.[2], with a magnetic field $B = 10$ T. Left: K valley. Right: K' valley.

defined. The higher Landau levels are less well defined, in agreement with the the fact that the description of a hopping modulation as an effective gauge field becomes exact only at the Dirac energy. The results are similar to those found in the analysis of the Quantum Hall Effect in thick nanotubes in a perpendicular field[25], where the (real) magnetic field is modulated and has zero total flux. There is a region in momentum space where the gaps between subbands have a minimum, corresponding to the region in real space where the effective field vanishes.

The effect of a uniform external magnetic field, which has the same sign for the two valleys, is shown in Fig.[3]. The combination of the breaking of inversion symmetry, induced by the ripple, and time reversal symmetry, induced by the magnetic field, leads to the inequivalence between the two valleys. The total effective field is greater in one than in the other, as shown by the larger region occupied by midgap states, and the fact that the higher bands show less dispersion. The results presented in Fig.[3] show that pseudomagnetic fields created by the ripples broaden all Landau levels except the zero-energy one. Interestingly, measurements of the activation gaps in the Quantum Hall Effect regime in graphene demonstrate that zero-energy Landau level is much narrower than the other ones [26]. The results obtained using this model are in agreement with calculations using the full valence band of graphene and the Local Density Functional Approximation for one dimensional ripples of smaller sizes[27].

Two dimensional ripples.

We consider now a single two dimensional ripple with axial symmetry. The elastic strains in circular coordinates are:

$$\begin{aligned} u_{rr} &= \partial_r u_r + (\partial_r h)^2 \\ u_{\theta\theta} &= \frac{\partial_\theta u_\theta}{r^2} + \frac{u_r}{r} + \frac{(\partial_\theta h)^2}{r^2} \\ u_{r\theta} &= \partial_r u_\theta + \frac{\partial_\theta u_r}{r} - \frac{u_\theta}{r} + \frac{\partial_r h \partial_\theta h}{r} \end{aligned} \tag{4}$$

The Dirac equation in radial coordinates is:

$$\begin{aligned} ie^{i\theta} v_{\rm F} \left(\partial_r + \frac{i\partial_\theta}{r} \right) \Psi_A(r,\theta) + t\beta e^{-2i\theta} \left(u_{rr} - u_{\theta\theta} - i u_{r\theta} \right) \Psi_A(r,\theta) &= \epsilon \Psi_B(r,\theta) \\ ie^{-i\theta} v_{\rm F} \left(\partial_r - \frac{i\partial_\theta}{r} \right) \Psi_B(r,\theta) + t\beta e^{2i\theta} \left(u_{rr} - u_{\theta\theta} + i u_{r\theta} \right) \Psi_B(r,\theta) &= \epsilon \Psi_A(r,\theta) \end{aligned} \tag{5}$$

where $\beta = \partial \log(t)/\partial \log(a)$, t is the hopping between nearest neighbor orbitals, and a is the distance between carbon atoms. If the gauge field induced by the ripple has circular symmetry, we obtain:

$$t\beta \left(u_{rr} - u_{\theta\theta} + i u_{r\theta} \right) = f(r) \tag{6}$$

A sketch of the ripples studied here is shown in Fig.[4], and also the associated effective magnetic field. The parameters used in the figure, $l = 600$Å and $h = 30$Å give a flux of effective magnetic field of order unity per ripple.

We compute numerically the electronic levels of ripples with axial symmetry, embedded in hexagons with periodic boundary conditions. The hexagons are labeled by an integer N, such that the total number of sites that they contain is $6(N*1)^2$. The side of the hexagon is $L = \sqrt{3}(N+1)a$, where $a = 1.4$Å is the distance between carbon atoms. The strains are simulated by an in plane deformation which modulates the hoppings:

$$t_{\vec{r}_i \vec{r}_j} = t_0 + t_0 \beta \frac{(\delta\vec{r}_i - \delta\vec{r}_j)\,(\vec{r}_i - \vec{r}_j)}{a^2} \tag{7}$$

with:

$$\delta\vec{r}_i = g(|\vec{r}_i|) \frac{\vec{r}_i}{|\vec{r}_i|} \tag{8}$$

and:

$$t\beta g(r) = A t r e^{-2(r/l)^2} \tag{9}$$

The resulting strain tensor is the same, in the continuum limit, to that is induced by a gaussian modulation of the height of the graphene sheet, $h(r) = h_0 e^{-(r/l)^2}$, with $A = \beta (h_0/l)^2$.

In the absence of the ripple, the levels have usually six- or twelvefold degeneracy, and are separated by gaps of order $v_{\rm F}/L$. There is a fourfold degenerate state at $E = 0$,

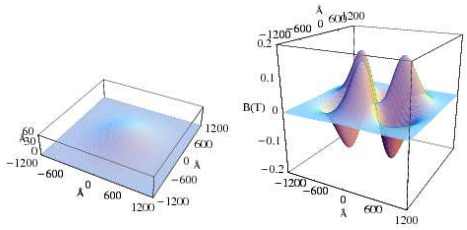

FIG. 4: (Color online). Right: Sketch of the ripple with an axially symmetric profile, similar to those analyzed in the text. The length is $l = 600$Å, and the height, is $h = 30$Å. Left: Effective magnetic field generated by the ripple, see text for details.

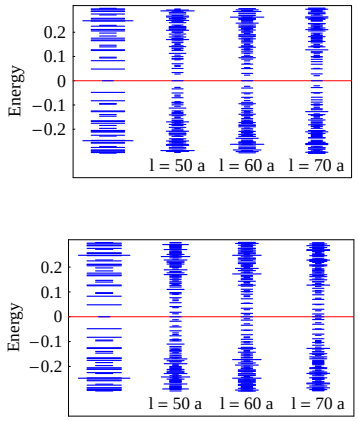

FIG. 5: (Color online). Energy levels (in units of t) for ripples with circular symmetry embedded in an hexagon with $6 \times 52^2 = 16224$ atoms and periodic boundary conditions, and different radii l (in units of a). The length of each line is proportional to the degeneracy of the level. Top: $A = 0.2$. Bottom: $A = 0.4$ (see text for details).

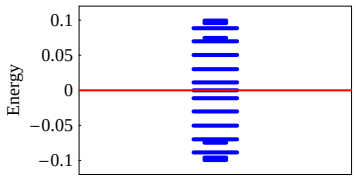

FIG. 6: (Color online). Low energy levels of the ripple with $A = 0.4$ and $l = 70a$ shown in Fig.[5].

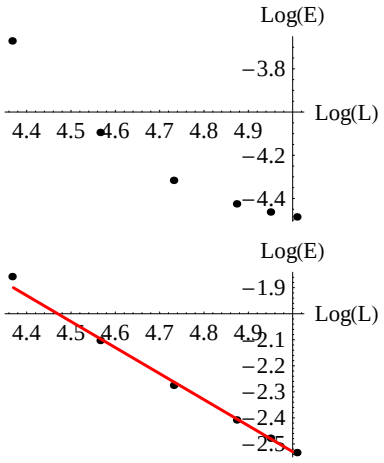

FIG. 7: (Color online). Top: Log-log plot of the scaling, as function of the size of the hexagon, of the lowest energy state away from $E = 0$ of a system with a ripple of radius $l = 50a$, and amplitude $A = 0.4$. Bottom: Scaling of the fifth level away from $E = 0$, and for the same parameters. The red straight line has a slope of -1.

as the number of unit cells in the hexagon is a multiple of three. The electronic spectra at low energies for hexagons with $N = 76$, (the number of sites is 34656) with embedded ripples of different sizes are shown in Fig.[5]. The side of these hexagons is $L \approx 131a \approx 18$nm. The ripple is defined as in eq.(9), with $A = 0.2$ and $A = 0.4$, and the radius of the ripple is $l = 50a, 60a$ and $70a$. The modified hoppings range from $0.9t$ to $1.2t$ for $A = 0.2$, and between $0.8t$ and $1.4t$ for $A = 0.4$.

In the presence of ripples, the degeneracy of the levels is reduced, and the number of low energy modes increases with the size of the ripple, in agreement with the analytical estimates made above. Note that there are still significant gaps between these states, indicating that they will lead to peaks in the density of states, and not to resonances within a broad continuum. The periodic boundary conditions imply that the low energy levels of a given ripple are hybridized with those in neighboring ones, leading to a shift from $E = 0$. The dependence of the level spacing with δt and l agrees with the estimates in Section IIa.

The low energy spectrum for a ripple of radius $l = 70a$ and amplitude $A = 0.4$ is shown in Fig.[6]. The level spacing near $E = 0$, $\Delta E \approx 0.02t$ implies an effective magnetic length, $l_B = v_F/\Delta E = (3ta/2)/\Delta E \approx 75a \sim l$. This length is larger, although the order of magnitude is comparable, than the analytical estimate obtained in Section IIa, $l_B \sim \sqrt{(t/\delta t)(la)} \sim \sqrt{70/0.3} \sim 15a$. Given the uncertainities associated to the estimate in Section IIa, and the fact that we have not taken into account that the effective field induced by the ripple is split into six peaks of smaller size than the ripple itself, we consider the agreement reasonable.

The scaling of the lowest level close to $E = 0$ as function of system size, L, for a fixed radius of the ripple, $l = 50a$, is shown in Fig.[7]. The energy scales approximately as L^{-1} for $l \lesssim L$, and it shows a weaker dependence on L for $l \ll L$. For comparison, the scaling of a level further away from $E = 0$ shows the L^{-1} scaling

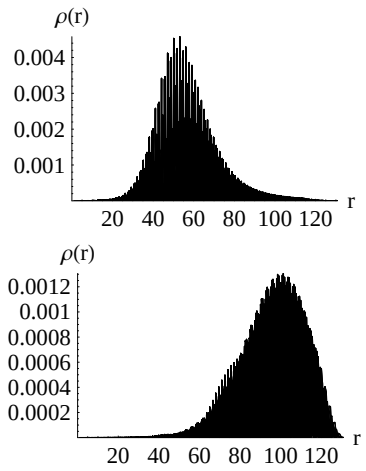

FIG. 8: (Color online). Top: Density profile of the wavefunction of the state closest to $E = 0$, of a ripple with radius $l = 50a$. The energy of this state is shown in Fig.[7]. Bottom: density for the fifth level away from $E = 0$.

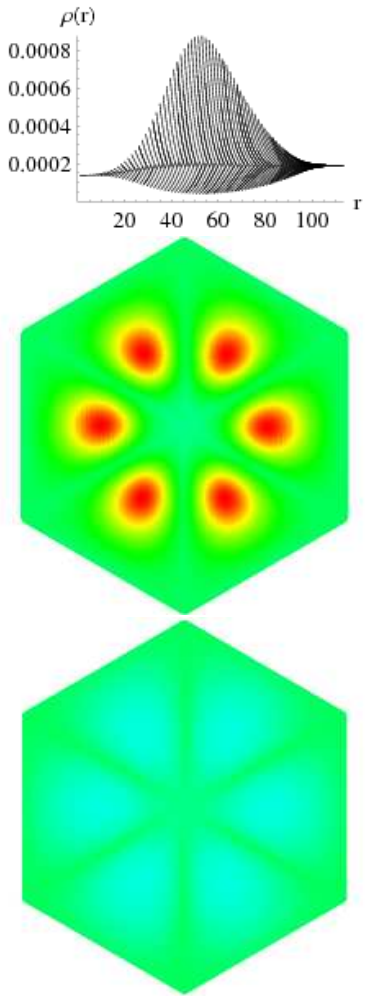

FIG. 9: (Color online). Top: Density as function of distance to the center of the wavefunction of the state at $E = 0$, of a ripple with radius $l = 50a$. Center: Density for sublattice A. Bottom: Density for sublattice B. The color code is such that density decreases from red to green, blue, and light blue.

as function of system size expected from a delocalized level described by the Dirac equation. The radial distribution of the density associated to these wavefunctions is shown in Fig.[8]. In agreement with the scaling behavior of the energy, one of the states is localized within the ripple, while the other is extended towards the edges of the hexagon.

All the lattices studied, with and without the modulation of the hoppings, show four zero energy states. In the clean system, the existence of these states is determined by the valley and sublattice degeneracy, and the density associated to them is uniform throughout the lattice. The spatial extent of these states changes qualitatively in the presence of a ripple, as shown in Fig.[9]. The wavefunctions become localized within the ripple, leading to a peak in the local density of states at $E = 0$, even if these states are delocalized. The wavefunction shows the hexagonal symmetry of the undelying lattice, and most of the charge is localized in six regions of the ripple. At the neutrality point there are only two (four including spin) electrons available in these states, opening the possibility of charge fractionalization.

The results presented above have been obtained for large modulations of the hoppings, or, alternatively, strong height corrugations. This limitation is imposed by the dimension of the hamiltonian which can be diagonalized.

The calculations show, however, that the low energy part of the spectra have the features expected from the continuum Dirac equation, and the wavefunctions associated to these states have a smooth envelope on scales comparable to the lattice constant. Hence, the method used can be considered a finite element technique which approximates well the Dirac equation in the presence of a ripple. The property of the lattice model which needs to be kept invariant is $v_{\rm F} = (3ta)/2$. The continuum equations are invariant under the scaling $l \to \lambda l$, $\delta t \to \delta t/\lambda$, and $E_n \to E_n/\lambda$. The scaling of δt implies that the corrugation of the ripple scales as $(h/l)^2 \to (h/l)^2/\lambda$. As a result, we can extrapolate the results analyzed here to ripples of larger size and weaker corrugations. The resulting effects are in agreement with the qualitative estimates made in Section IIa.

INTERACTION EFFECTS.

The analysis in the preceding section shows that rippled graphene samples, in the absence of interactions, have a peak in the density of states at the Dirac energy. The width of this peak decreases as $e^{-(\delta t/t)(l/a)}$, and the

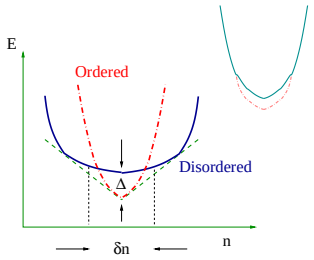

FIG. 10: (Color online). Sketch of the free energy of an ordered phase induced by interactions. The ordered phase is assumed to have a gap, and the derivative of the free energy at $n = 0$ is discontinuous. On the other hand, the disordered phase is assumed to have a high electronic compressibility. The Maxwell construction indicated by the straight lines shows the region where electronic phase separation occurs. For comparison, an ordinary second order phase transition between phases with similar electronic compressibilities is also shown. See text for details.

fraction of states, in an area of size l^2, that it includes is proportional to the same dimensionless combination, $f \sim (\delta t/t)(l/a)$. The resulting diverging electronic compressibility implies that interactions will induce instabilities, in the same way as in graphene in a magnetic field near half filling[28, 29, 30, 31, 32, 33, 34, 35]. As shown in Fig.[2], while the midgap states are well defined, the higher bands, for small values of $\delta t/t$, tend quickly towards the clean graphene limit. If the interactions are weak, this implies that their effect is limited to the states within a narrow range of energies near the neutrality point. Alternatively, it can be argued that interactions can be studied in a restricted hamiltonian which includes only the midgap states. Hence, a reasonable upper bound to the gap opened by many body effects is $\Delta \sim \sqrt{(t\delta t)(a/l)}$.

A plausible ordered phase which can emerge at low temperatures is a ferromagnetic phase[30, 32]. The saturation magnetization will be small, $m \sim (\delta t/t)/(al)$. The Curie temperature needs not be small, as transverse spin waves in a system like this do not induce a large suppression of T_C[36]. This phase may help to explain the observation of ferromagnetism in graphite samples[37].

Phase transitions in systems where the electronic compressibility is large are often of first order, and the system has a tendency towards electronic phase separation in the ordered phase[38, 39]. The expected dependence of the free energy of the ordered and disordered phases as function of electronic concentration is sketched in Fig.[10]. The region of phase separation which can be obtained from a Maxwell interpolation using the free energies of the different phases will be replaced by a disordered phase with charge puddles, as the long range Coulomb interaction suppresses macroscopic phase separation. The resulting situation resembles that in magnetic systems with striped phases or domains[40, 41].

We can make a qualitative estimate of the sizes of the charge puddles by comparing the energy gain per unit area in the ordered phase and the electrostatic cost of forming the puddle. For a puddle of size L_{pud}, the energy in the ordered phase decreases by an amount $\Delta n L_{pud}^2$, where n is the density of electrons contribute to the ordered phase. The electrostatic energy is $e^2 n^2 L_{pud}^3$. Then, the typical puddle size is $L_{pud} \sim \Delta/(e^2 n)$. Putting together the estimates made above, we obtain:

$$\begin{aligned} \Delta &= \sqrt{\frac{t\delta t a}{l}} \\ n &= \frac{\delta t}{t}\frac{1}{la} \\ L_{pud} &= l\frac{ta}{e^2}\sqrt{\frac{t}{\delta t}\frac{l}{a}} \sim l\frac{v_F}{e^2}\sqrt{\frac{t}{\delta t}\frac{a}{l}} \end{aligned} \qquad (10)$$

As in graphene $e^2/v_F \sim 1$, and $\sqrt{\frac{t}{\delta t}\frac{a}{l}} \sim O(1)$ for reasonable ripple parameters, the size of the puddle will be comparable with that of the ripple. A sketch of the gap opened by an periodic electrostatic potential, $v(x,y) = v_0 \sin(2\pi x/l)$, with $v_0 = 0.02$eV is shown in the bottom right graph in Fig[2]. The gap is of the same order of magnitude as the amplitude of the potential.

CONCLUSIONS.

We present analysis of the changes in the electronic structure of graphene due to modulations in the hoppings induced by ripples and other sources of elastic strains. The changes in the electronic structure are determined by the dimensionless parameter $\Phi \sim (\delta t/t)(l/a) \sim (\delta v_F/v_F)(l/a) \sim (\beta h^2)/(la)$, where $\delta t/t = \delta v_F/v_F$ is the modulation of the hopping parameter, or the Fermi velocity, v_F, h is the height of the rippls, l is the size of the ripple, and a is the lattice constant. The parameter Φ gives the flux of effective magnetic field threading an area of the size of the ripple.

We find that reasonable values for the size and height of a ripple lead to the formation of midgap states. These midgap states are similar to the Landau levels at the Dirac energy induced by a magnetic field. The combination of hopping modulations and a magnetic field breaks the symmetry between the two graphene valleys, leading to the possibility of valley selection[42], as electrons from each valleys will scatter differently from extended defects[43].

Midgap states induce a large electronic compressibility when the Fermi energy is near the Dirac point. Interaction effects will lead to instabilities towards ordered phases, and electronic phase separation, with typical puddle size not too different from that of the ripple.

ACKNOWLEDGMENTS.

We thank L. Brey, P. le Doussal, A. Castro Neto, A. K. Geim, J. González, B. Horovitz, and K. S. Novoselov for useful conversations. This work was supported by MEC (Spain) through grant FIS2005-05478-C02-01, the Comunidad de Madrid, through the program CITECNOMIK, CM2006-S-0505-ESP-0337, the European Union Contract 12881 (NEST)(F. G. and M. A. H. V.) and by FOM (Netherlands) (M. K.).

APPENDIX. ANALYTICAL MODELS OF LOW ENERGY STATES IN RIPPLED GRAPHENE.

Straight ripple.

We analyze simple models of elastic deformations and the midgap states that they may induce.

We study first a straight boundary between a stretched and a relaxed region in graphene, as schematically shown in Fig.[11]. We describe the change in the stretched region by a change in the nearest neighbor hopping, t, along the horizontal direction, $t + \delta t$.

The Dirac hamiltonian in the stretched region, is:

$$\mathcal{H} \equiv \begin{pmatrix} 0 & v_{\rm F}(-ik_x \mp k_y) + \delta t \\ v_{\rm F}(k_x \mp k_y + \delta t) & 0 \end{pmatrix} \quad (11)$$

so that the perturbation induces a gauge field in the y direction, A_y. At the boundary, we have $\partial_x A_y \neq 0$.

The system has translational symmetry along the y axis, so that k_y is conserved. The Dirac equation, for a given valley reads:

$$\begin{aligned} v_{\rm F}\partial_x \psi_A(x) \pm (v_{\rm F} k_y \mp \delta t(x))\psi_A(x) &= \epsilon \psi_B(x) \\ -v_{\rm F}\partial_x \psi_B(x) \pm (v_{\rm F} k_y \mp \delta t(x))\psi_B(x) &= \epsilon \psi_A(x) \end{aligned} \quad (12)$$

These set of equations give the one dimensional Dirac equation with a gap $\Delta(x) = v_{\rm F} k_y + \delta t(x)$. If the gap changes sign across the interface they have localized solutions at $\epsilon = 0$. This condition implies that either $v_{\rm F} k_y > 0$ and $v_{\rm F} k_y + \delta t < 0$ or $v_{\rm F} k_y < 0$ and $v_{\rm F} k_y + \delta t > 0$. Irrespective of the sign of δt, there is a range of values of k_y:

$$\delta k_y = \frac{|\delta t|}{v_{\rm F}} \quad (13)$$

The electronic structure of the system is schematically shown in Fig.[12]. The distortion shifts the Dirac cone in the stretched region. A band of localized states joining the two Dirac cones is induced. The number of midgap states per unit length of the ripple is:

$$n_{1D} = \frac{8|\delta t|}{3ta} \quad (14)$$

where t is the nearest neighbor hopping, and a is the $C - C$ distance.

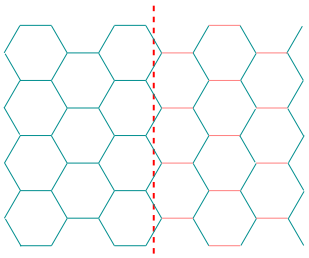

FIG. 11: (Color online). Sketch of a boundary between a stretched and a relaxed region of graphene.

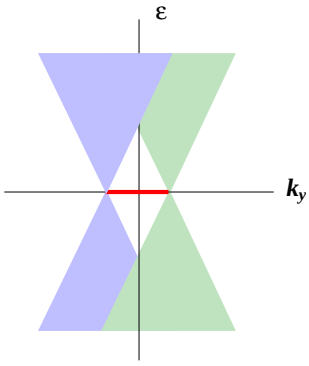

FIG. 12: (Color online). Electronic spectrum as function of k_y of the interface shown in Fig.[11].

Circular ripple.

The zero energy wavefunction in a given valley, in the presence of a circular ripple, obeys the Dirac equation, eq.(5):

$$ie^{i\theta} v_{\rm F} \left(\partial_r + \frac{i\partial_\theta}{r} \right) \Psi_A(r,\theta) + f(r) e^{-2i\theta} \Psi_A(r,\theta) = 0 \quad (15)$$

and related equations for $\Psi_B(r,\theta)$ and for the other valley. This equation can be integrated analytically, and we obtain:

$$\Psi(r,\theta) = f(re^{i\theta}) e^{i \frac{e^{-3i\theta}}{v_{\rm F} r^3} \int_0^r dr' r'^3 f(r')} \quad (16)$$

where $f(z)$ is an analytic function. This wavefunction is not normalizable, irrespective of the choice of $f(z)$. Choosing $f(re^{i\theta}) = A$, where A is a constant, the electronic density is:

$$\rho(r,\theta) = A^2 e^{\frac{2\sin(3\theta)}{v_{\rm F} r^3} \int_0^r dr' r'^3 f(r')} \quad (17)$$

Assumming, for instance, that $\lim_{r\to\infty} f(r) \sim O\left(e^{-2(r/l)^2}\right)$,and that $f(r)$ does not diverge as $r \to 0$, we find:

$$\begin{aligned} \lim_{r\to 0} \rho(r,\theta) &= A^2 \\ \lim_{r\to\infty} \rho(r,\theta) &= A^2 \end{aligned} \quad (18)$$

The density has maxima at for a radial coordinate comparable to the radius of the ripple, $r \sim l$, where it depends exponentially on a quantity of order $f(l)l/v_{\rm F} \sim \beta h^2/(la)$. As a function of θ, $\rho(r \sim l, \theta)$ has three maxima and three minima.The positions of the maxima and the minima are interchanged when analyzing the other valley. The resulting pattern is in good agreement with the numerical results shown in Fig.[9].

[1] K. S. Novoselov, D. Jiang, F. Schedin, T. J. Booth, V. V. Khotkevich, S. V. Morozov, and A. K. Geim, Proc. Nat. Acad. Sc. **102**, 10451 (2005).

[2] A. K. Geim and K. S. Novoselov, Nature Materials **6**, 183 (2007).

[3] J. C. Meyer, A. K. Geim, M. I. Katsnelson, K. S. Novoselov, T. J. Booth, and S. Roth, Nature **446**, 60 (2007).

[4] E. Stolyarova, K. T. Rim, S. Ryu, J. Maultzsch, P. Kim, L. E. Brus, T. F. Heinz, M. S. Hybertsen, and G. W. Flynn, Proc. Natl. Acad. Sci. USA **104**, 9209 (2007).

[5] M. Ishigami, J. H. Chen, W. G. Cullen, M. S. Fuhrer, and E. D. Williams, Nano Letters (2007).

[6] A. Fasolino, J. H. Los, and M. I. Katsnelson, Nature Mat. **6**, 858 (2007).

[7] J. González, F. Guinea, and M. A. H. Vozmediano, Phys. Rev. Lett. **69**, 172 (1992).

[8] J. González, F. Guinea, and M. A. H. Vozmediano, Nucl. Phys. B **406 [FS]**, 771 (1993).

[9] A. Morpurgo and F. Guinea, Phys. Rev. Lett. **97**, 196804 (2006).

[10] A. Cortijo and M. A. H. Vozmediano, Europhys. Lett. **77**, 47002 (2007).

[11] F. de Juan, A. Cortijo, and M. A. H. Vozmediano, Phys. Rev. B **76**, 165409 (2007).

[12] H. Suzuura and T. Ando, Phys. Rev. B **65**, 235412 (2002).

[13] S. V. Morozov, K. S. Novoselov, M. I. Katsnelson, F. Schedin, L. A. Ponomarenko, D. Jiang, and A. K. Geim, Phys. Rev. Lett. **97**, 016801 (2006).

[14] J. L. Mañes, Phys. Rev. B **76**, 045430 (2007).

[15] A. H. Castro Neto and E.-A. Kim (2007), arXiv:cond-mat/0702562.

[16] E. McCann, K. Kechedzhi, V. I. Fal'ko, H. Suzuura, T. Ando, and B. L. Altshuler, Phys. Rev. Lett. **97**, 146805 (2006).

[17] R. V. Gorbachev, F. V. Tikhonenko, A. S. Mayorov, D. W. Horsell, and A. K. Savchenko, Phys. Rev. Lett. **98**, 176805 (2007).

[18] X. Wu, X. Li, Z. Song, C. Berger, and W. A. de Heer, Phys. Rev. Lett. **98**, 136801 (2007).

[19] F. V. Tikhonenko, D. W. Horsell, R. V. Gorbachev, and A. K. Savchenko (2007), arXiv:0707.0140.

[20] J. Martin, N. Akerman, G. Ulbricht, T. Lohmann, J. H. Smet, K. von Klitzing, and A. Yacoby, Nature Physics (2007), online publication, doi:10.1038/nphys781.

[21] N. M. R. Peres, F. Guinea, and A. H. Castro Neto, Physical Review B **73**, 125411 (2006).

[22] K. S. Novoselov, A. K. Geim, S. V. Morozov, D. Jiang, M. I. Katsnelson, I. V. Grigorieva, S. V. Dubonos, and A. A. Firsov, Nature **438**, 197 (2005).

[23] R. Jackiw, Phys. Rev. D **29**, 2375 (1984).

[24] B. Horovitz and P. le Doussal, Phys. Rev. B **65**, 125323 (2002).

[25] E. Perfetto, J. González, F. Guinea, S. Bellucci, and P. Onorato, Phys. Rev. B **76**, 125430 (2006).

[26] A. J. M. Giesbers, U. Zeitler, M. I. Katsnelson, L. A. Ponomarenko, T. M. Ghulam, and J. C. Maan, Phys. Rev. Lett. **99**, 206803 (2007).

[27] T. O. Wehling, A. V. Balatsky, M. I. Katsnelson, and A. I. Lichtenstein (2007), arXiv:0710.5828.

[28] V. P. Gusynin, V. A. Miransky, S. G. Sharapov, and I. A. Shovkovy, Phys. Rev. B **74**, 195429 (2006).

[29] M. O. Goerbig, R. Moessner, and B. Doučot, Phys. Rev. B **74**, 161407 (2006).

[30] K. Nomura and A. H. MacDonald, Phys. Rev. Lett. **96**, 256602 (2006).

[31] H. A. Fertig and L. Brey, Phys. Rev. Lett. **97**, 116805 (2006).

[32] J. Alicea and M. P. A. Fisher, Phys. Rev. B **74**, 075422 (2006).

[33] J.-N. Fuchs and P. Lederer, Phys. Rev. Lett. **98**, 016803 (2007).

[34] D. A. Abanin, K. S. Novoselov, U. Zeitler, P. A. Lee, A. K. Geim, and L. S. Levitov, Phys. Rev. Lett. **98**, 196806 (2007).

[35] V. Lukose and R. Shankar (2007), arXiv:0706.4280.

[36] D. M. Edwards and M. I. Katsnelson, J. Phys.: Condens. Matter **18**, 31 (2006).

[37] P. Esquinazi, D. Spemann, R. Höhne, A. Setzer, K.-H. Han, and T. Butz, Phys. Rev. Lett. **91**, 227201 (2003).

[38] F. Guinea, G. Gómez-Santos, and D. P. Arovas, Phys. Rev. B **62**, 391 (2002).

[39] B. Spivak, Phys. Rev. B **93**, 125205 (2004).

[40] R. Brucas, H. Hafermann, M. I. Katsnelson, I. L. Soroka, O. Eriksson, and B. Hjrvarsson, Phys. Rev. B **69**, 064411 (2004).

[41] P. A. Prudkovskii, A. N. Rubtsov, and M. I. Katsnelson, Europhys. Lett. **73**, 104 (2006).

[42] A. Rycerz, J. Tworzydo, and C. W. J. Beenakker, Nature Physics **3**, 172 (2007).

[43] V. V. Cheianov and V. I. Fal'ko, Phys. Rev. B **74**, 041403 (2006).